Rotating machinery reliability assessment based on improved extreme learning machine and hippopotamus optimization algorithm

Muhammad Firdaus Bin Isham[1]* , Muhammad Harith Mohd Kamal[1] ,
Amirulaminnur Raheimi[2] , Mohd Syahril Ramadhan Mohd Saufi[1],
Meng Hee Lim[2], Muhd Salman Leong[2], Nur Fathiah Waziralilah[3]

[1] Faculty of Mechanical Engineering, Universiti Teknologi Malaysia, Johor, 81310, Malaysia
[2] Institute of Noise and Vibration, Universiti Teknologi Malaysia, Kuala Lumpur, 54100, Malaysia
[3] Mechanical Engineering Department, Alfaisal University, Riyadh, 11533, Saudi Arabia
* Corresponding author's e-mail: mfirdausisham@gmail.com

ABSTRACT

The utilisation of rotating machinery across diverse industrial applications underscores the critical importance of evaluating its reliability to ensure the safe operation of these systems. Bearings, as fundamental components within engineering facilities, hold particular significance; their malfunction can result in severe safety incidents, heightened maintenance expenditures, and considerable economic consequences. Extreme learning machine (ELM) represents a machine learning approach that proficiently addresses numerous challenges inherent in conventional machine learning algorithms. Nonetheless, the efficacy of the ELM may deteriorate and yield inaccurate results due to an inappropriate use of its parameters, which include input weights, biases, and the number of hidden neurons. This paper proposes an improved ELM (IELM) model that incorporates the Hippopotamus optimization algorithm (HOA) to optimise the parameters and enhance the performance of the ELM in rotating machinery reliability assessment. Initially, the HOA method is employed to identify optimised parameter values for the ELM. Subsequently, these optimised values are integrated into the proposed IELM-HOA framework for the purpose of fault classification. This study utilises time-domain statistical features to extract significant information from the vibration signals. The dataset comprises vibration signals derived from both online bearing datasets and experimental bearing datasets. The findings indicate that the proposed IELM-HOA method enhances the performance of the ELM technique. Furthermore, it demonstrates the capability to exceed and compete with recently introduced fault diagnosis methodologies.

Keywords: reliability assessment, ELM, bearing, vibration signal, meta-heuristic.

INTRODUCTION

The reliability of rotating machinery plays a pivotal role in numerous industrial applications, as it has a direct impact on operational efficiency, safety, and maintenance expenses. In any machinery, components such as bearings and gears endure substantial wear and tear, alongside the risk of operational failures [1–4]. These critical elements function under challenging conditions, where variables such as friction, fluctuations in temperature, and load stresses may contribute to their gradual deterioration over time. The incessant operational cycle of machinery exerts significant strain on these parts, culminating in progressive degradation. Therefore, it is imperative to routinely monitor and assess their performance. The early identification of wear or potential faults can avert catastrophic failures, thereby ensuring efficient operation and extending the lifespan of the equipment. Appropriate maintenance strategies should be employed to mitigate these risks and preserve the integrity of these essential components. State-of-the-art approach, including the IELM in conjunction with the HOA, offer innovative strategies to enhance

the predictive accuracy of reliability assessments. By incorporating these advanced techniques, we can substantially elevate our capacity to detect potential failures and optimise maintenance approaches, thereby ensuring the durability and performance of rotating machinery across various operational settings.

The traditional approach to fault diagnosis predominantly utilises analytical redundancy and gradient-based learning techniques, including feedforward neural networks that modify their parameters through iterative methods. This strategy frequently results in prolonged training times and can give rise to overfitting due to the intricacy of the models used. Moreover, conventional feature extraction techniques often necessitate specialised knowledge, thereby constraining their applicability in various diagnostic investigations [5, 6]. Such methods typically encounter difficulties associated with limited data and imbalanced datasets, especially in industrial contexts where certain fault states are under-represented [7]. Additionally, traditional feature selection methodologies may produce larger subsets of features that are less relevant, thereby diminishing diagnostic efficacy [8]. The shortcomings of these conventional approaches have led to an increasing enhancement or replacement of methods by data-driven strategies that leverage artificial intelligence to boost efficiency. This has spurred the investigation of more effective alternatives, such as the ELM, which provides rapid learning and enhanced generalisation capabilities, thus addressing the deficiencies inherent in conventional techniques [9, 10].

The ELM method, introduced by Huang et al. in 2006, has attracted significant attention from various researchers and practitioners [11]. This interest can be attributed to its ability to resolve shortcomings associated with traditional machine learning algorithms, such as artificial neural networks (ANN) and support vector machines (SVM). The ELM method has been thoroughly investigated and applied across numerous domains, including medicine [12], structural engineering [13], geology [14], and rotating machinery [15]. Nevertheless, the performance and stability of the ELM approach can suffer when its three critical parameters—input weights, biases, and the number of hidden neurons—are inaccurately specified. Consequently, a range of optimisation techniques have been integrated into ELM to enhance its stability and classification precision. For instance,

Meng et al. and Guo et al. employed genetic algorithms (GA) to optimise ELM for bearing diagnostics [16, 17]. Isham et al. optimised the ELM method through different studies, using the geometric mean optimiser (GMO) and the whale optimisation algorithm (WOA) for diagnosing gears and bearings [18, 19]. Wang et al. introduced an ELM framework enhanced by improved particle swarm optimisation (PSO) for bearing diagnostics [20]. Similarly, Sun et al. utilised the GWO to optimise ELM parameters for machinery fault detection based on vibration signals [21]. Research into ELM parameter optimisation remains ongoing, with numerous new optimisation algorithms and meta-heuristic methods being incorporated to evaluate their effectiveness.

Consequently, this study introduces a novel and effective optimisation technique for determining the optimal parameters of the ELM through a recently developed meta-heuristic method referred to as the HOA, also identified as IELM-HOA. The HOA is a novel meta-heuristic algorithm inspired by the hunting behaviour of hippos in their natural habitat. Designed for efficiency and robustness, HOA aims to optimise various parameters in complex problems by mimicking the strategies employed by these animals during foraging. Research on the HOA method continues to be limited, as it is a relatively new technique. This study seeks to employ the HOA method to identify and determine the optimal parameters for the ELM, with the aim of enhancing its performance and improving the consistency of classification outcomes. The proposed Integrated ELM-HOA (IELM-HOA) will be assessed using two distinct datasets concerning bearings, which will be thoroughly presented and analysed within this paper. Therefore, the aims of this paper are: 1) to make a substantial contribution to the field of fault diagnosis by introducing an innovative approach to the reliability assessment of rotating machinery, referred to as IELM-HOA, and 2) to further the discipline of machine learning by refining the conventional ELM method to achieve increased stability and efficacy.

This paper is structured as follows. First, a brief overview of the Hippopotamus optimisation algorithm will be provided. Next, the proposed IELM-HOA will be detailed, followed by a comprehensive description of the experimental setup and results. Finally, a discussion of the findings will be presented, and the paper will conclude with a summary and suggestions for future research.

THEORETICAL BACKGROUND

Hippopotamus optimization algorithm

The Hippopotamus optimization algorithm is a novel approach inspired by the behavior and habitat of hippopotamuses. This algorithm is designed to address optimization problems by simulating the natural movement and foraging behaviors of these animals in their ecosystems. HOA utilizes a population-based method where potential solutions are represented as a group of hippos. The algorithm's initialization phase involves randomly distributing these hippos in the solution space, allowing them to explore various regions. Throughout the optimization process, hippos interact with one another, sharing information about their respective positions and the quality of their solutions. the initialization stage of the HO involves generating randomized initial solutions. During this phase, the vector of decision variables is formulated using the subsequent formula presented as Eq. 1, where X_i represent the position of the candidate solution, r is a random number in the range of 0 to 1, N is a population size, and m is a problem dimension.

$$X_i: x_{ij} = lb_j + r.\left(ub_j - lb_j\right)$$
$$i = 1,2 \ldots, N, j = 1,2, \ldots, m \tag{1}$$

The algorithm incorporates various strategies such as migration and local search, which enhance the search capabilities by allowing hippos to move toward better solutions while maintaining diversity within the population. This balance between exploration and exploitation is crucial for avoiding local optima and improving overall solution quality. Phase 1 for exploration, the dominant male hippopotamuses are determined through an objective function value iteration process, ensuring territory and herd protection, while expelled males must either attract females or compete for dominance to establish their status. Equation 2 mathematically represents the spatial positioning of male hippopotamus individuals within the herd in a lake or pond environment, where X_i^{Mhippo} is a male hippopotamus position, D_{hippo} is the dominant hippopotamus position.

$$X_i^{Mhippo}: x_{ij}^{Mhippo} = x_{ij} + y_1.\left(D_{hippo} - I_1 x_{ij}\right)$$
$$for\ i = 1,2, \ldots, \left[\frac{N}{2}\right] and\ j = 1,2, \ldots m \tag{2}$$

Equation 3 quantify the positioning of female or immature hippopotamuses within the herd,

indicating that a T value exceeding 0.6 signifies a notable separation from their mothers, typically resulting from curiosity-driven behaviour. Equation 4 illustrate the positional adjustments of both male and female, as well as juvenile, hippopotamuses within the herd, where F_i is an objective function.

$$X_i^{FBhippo}: X_{ij}^{FBhippo} =$$
$$= \begin{cases} x_{ij} + h_1.\left(D_{hippo} - I_2 MG_i\right) & T > 0.6 \\ \Xi & else \end{cases} \tag{3}$$

$$X_i = \begin{cases} X_i^{HippoR} & F_i^{HippoR} < F_i \\ X_i F_i^{HippoR} & \geq F_i \end{cases} \tag{4}$$

Phase 2 for exploration where hippopotamuses protect themselves from predators. Equation 5 represent the predator's position in search space and Eq. 6 is a distance between hippopotamus with the predator respectively.

$$Predator: Predator_j =$$
$$= lb_j + \vec{r}_8.\left(ub_j - lb_j\right), j = 1,2, \ldots, m \tag{5}$$

$$\vec{D} = \left|Predator_j - x_{ij}\right| \tag{6}$$

Phase 3 pertains to the exploitation stage, characterized by the hippopotamus evading its predator. In response to encountering a group of predators or being unable to effectively defend itself, a hippopotamus typically seeks refuge in nearby lakes or ponds, where it can evade threats from spotted lions and hyenas, thereby improving its local search capabilities as reflected in Phase Three of the HO results. These presented in Equations 7 and 8 respectively.

$$lb_j^{local} = \frac{lb_j}{t}, ub_j^{local} =$$
$$= \frac{ub_j}{t}, t = 1,2, \ldots, \tau \tag{7}$$

$$X_i = \begin{cases} X_i^{HippoE} & F_i^{HippoE} < F_i \\ X_i F_i^{HippoE} & \geq F_i \end{cases} \tag{8}$$

In summary, the HOA combines biological inspiration with computational techniques to efficiently tackle complex optimization challenges. Its unique approach provides a fresh perspective in the field of optimization algorithms. The flowchart of the HOA algorithm presented in Figure 1.

The proposed IELM-HOA algorithm

Extreme learning machine represents a straightforward yet highly effective learning methodology specifically designed for single-hidden layer feedforward neural networks (SLFNs), thereby offering a practical
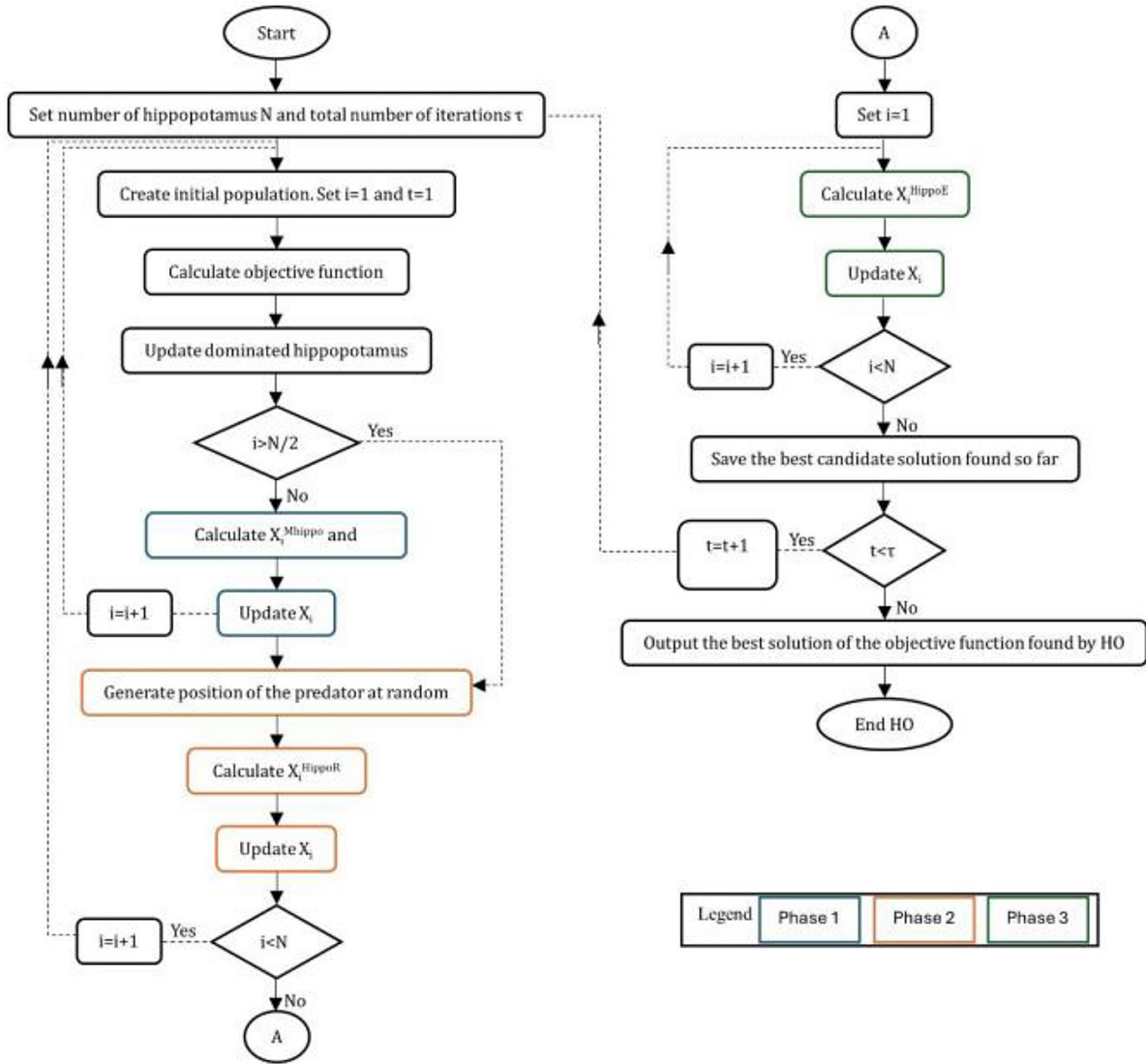
Figure 1. HOA flowchart

and efficient alternative to traditional artificial neural networks (ANNs) as well as support vector machines (SVMs). Within the conventional ELM framework, the input weights and hidden layer biases are randomly assigned values within a specified range of 0 to 1 during the computational process, which can influence overall performance. Moreover, the number of hidden neurons is generally determined in relation to the number of input features, as has been established by various researchers in the field. Unfortunately, these predetermined sets of parameters have often led to notable performance degradation and inconsistencies in results. To address these challenges and enhance the overall performance of the ELM method, the HOA is employed to systematically optimize the values that will be utilized for input weights, biases, and the configuration of hidden neurons. The detailed flowchart of the proposed methodological approach is expediently presented in Figure 2.

This study utilizes two distinct sets of bearing datasets, namely the CWRU bearing datasets, which are sourced from online repositories, and experimental datasets. These datasets were organized into signal samples, from which statistical features were subsequently extracted from each sample. The extracted features for each signal sample were then arranged into two configurations intended for the optimization and classification processes. Equation 9 details the objective function for the HOA.

$$Obj. Function = 100 - \left[\frac{Training\ Acc.\,(\%) + Testing\ Acc.\,(\%)}{2} \right] \quad (9)$$
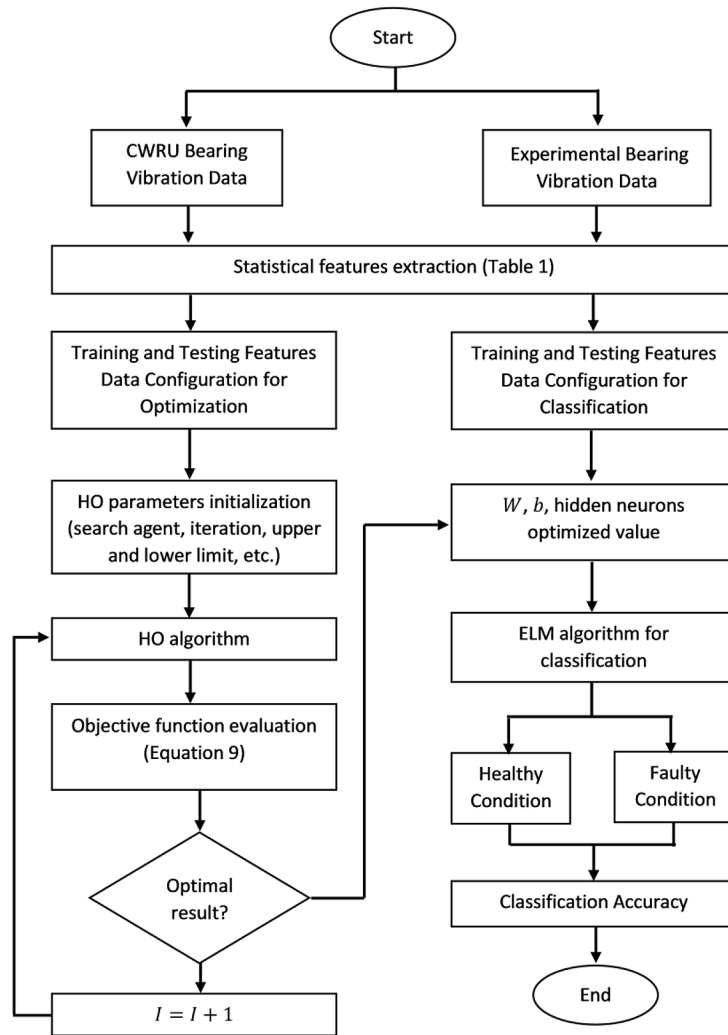
Figure 2. IELM-HOA flowchart

METHODOLOGY

This study employs two categories of vibration datasets: (1) the Case Western Reserve University (CWRU) bearing datasets, and (2) experimental bearing datasets. The CWRU bearing datasets are publicly available and consist of four distinct conditions of ball bearing vibrations: healthy, ball fault, inner race fault, and outer race fault, as illustrated in Figure 3a. The

Figure 3. (a) CWRU datasets and (b) experimental datasets

motor operates at a speed of 1797 RPM with a sampling frequency of 12 kHz, and the fault size is approximately 0.040 inches (around 1.0 mm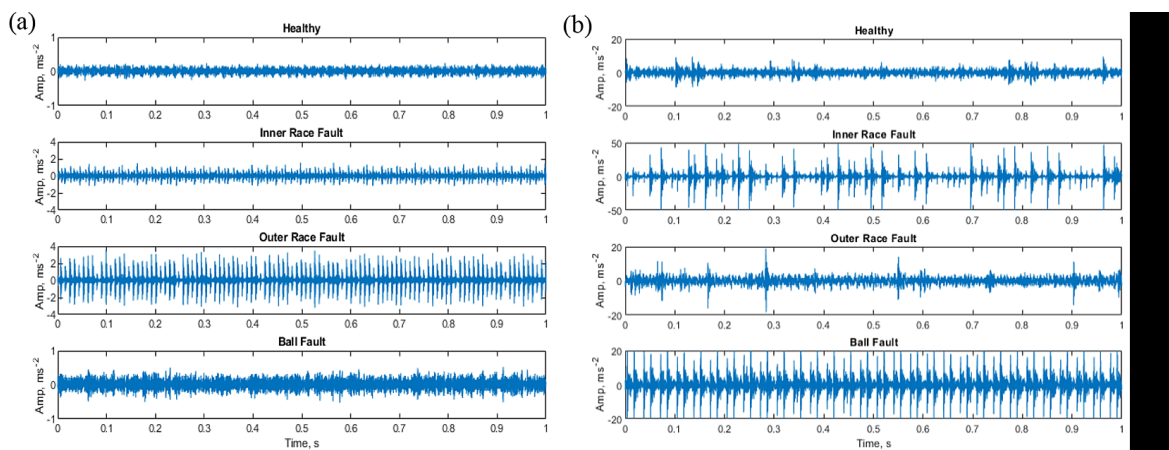). This study used an experimental dataset that included four distinct conditions: healthy, ball fault, inner race fault, and outer race fault. The test rig utilized was the SpectraQuest Machinery Fault and Rotor Dynamics Simulator (MFS-RDS), with the complete experimental setup and configuration, including sensors and analyzer, illustrated in Figure 3b. The experiment was conducted with the motor operating at a speed of 1800 RPM, a sampling frequency of 25.6 kHz, and a fault size of approximately 1.5 mm. The complete experimental setup is shown in Figure 4, respectively.

Then, all the vibration signals from each dataset are sampled according to their revolution per second. The eight time-domain statistical features listed in Table 1 were then extracted from each signal sample, where $x(i)$ is a time-series signal. Table 2 summarizes the distribution of the signal sample data for training and testing. Configuration D1 and D3 are specifically for fault classification and diagnosis using CWRU datasets and experimental datasets, respectively. The configurations D2 and D4 are specifically for parameter optimization purposes. This is due to the objective function for the HOA algorithm, which reflects the accuracy of the ELM method as presented in Equation 9.
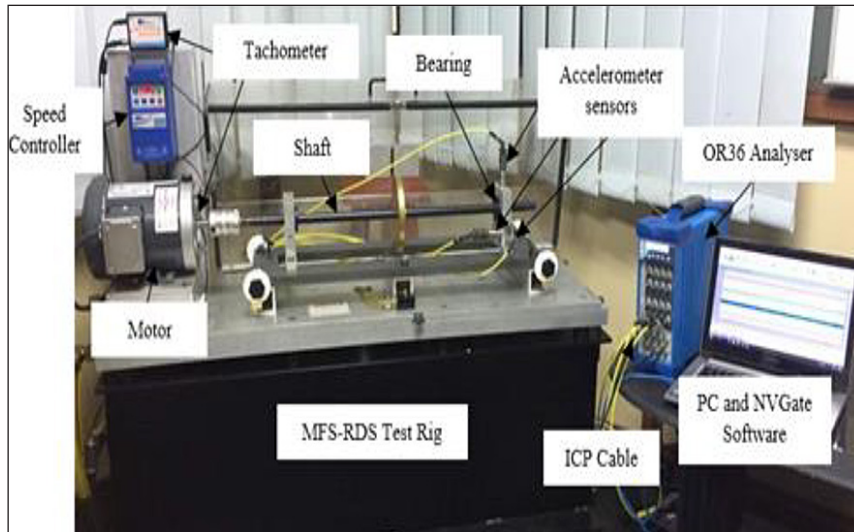
Figure 4. Experimental setup

Table 1. Vibration time-domain statistical features

Statistical feature	Equation	Statistical feature	Equation
Range	$\max(x_i) - \min(x_i)$	Crest factor	$\dfrac{max\|x_i\|}{\sqrt{\frac{1}{N}\Sigma_{i=1}^{I} x_i^2}}$
RMS	$\sqrt{\dfrac{\Sigma_{i=1}^{I} x_i^2}{N}}$	Shape factor	$\dfrac{\sqrt{\frac{1}{N}\Sigma_{i=1}^{I} x_i^2}}{\frac{1}{N}\Sigma_{i=1}^{I}\|x_i\|}$
Skewness	$\dfrac{\frac{1}{N}\Sigma_{i=1}^{I}(x_i - \bar{x})^3}{\left(\sqrt{\frac{1}{N}\Sigma_{i=1}^{I}(x_i - \bar{x})^2}\right)^3}$	Impulse factor	$\dfrac{max\|x_i\|}{\frac{1}{N}\Sigma_{i=1}^{I}\|x_i\|}$
Kurtosis	$\dfrac{\frac{1}{N}\Sigma_{i=1}^{I}(x_i - \bar{x})^4}{\left(\sqrt{\frac{1}{N}\Sigma_{i=1}^{I}(x_i - \bar{x})^2}\right)^4}$	Margin factor	$\dfrac{max\|x_i\|}{\left(\frac{1}{N}\Sigma_{i=1}^{I}\sqrt{\|x_i\|}\right)^2}$

Table 2. Signal sample data distribution for training and testing

Configuration	Training sample	Testing sample	Condition	Label
D1	120 × 8	30 × 8	Healthy	0.2
	120 × 8	30 × 8	Inner race fault	0.4
	120 × 8	30 × 8	Outer race fault	0.6
	120 × 8	30 × 8	Ball fault	0.8
D2	60 × 8	15 × 8	Healthy	0.2
	60 × 8	15 × 8	Inner race fault	0.4
	60 × 8	15 × 8	Outer race fault	0.6
	60 × 8	15 × 8	Ball fault	0.8
D3	160 × 8	40 × 8	Healthy	0.2
	160 × 8	40 × 8	Inner race fault	0.4
	160 × 8	40 × 8	Outer race fault	0.6
	160 × 8	40 × 8	Ball fault	0.8
D4	80 × 8	20 × 8	Healthy	0.2
	80 × 8	20 × 8	Inner race fault	0.4
	80 × 8	20 × 8	Outer race fault	0.6
	80 × 8	20 × 8	Ball fault	0.8

RESULS

Parameter optimization for ELM

The ELM parameters, which are input weight, bias, and hidden neurons, will be optimized in this section based on the HOA algorithm. Signal configuration presented in Table 2, D2 (CWRU datasets) and D4 (experimental dataset) are used for this purpose. In order to run the HOA algorithm, the initial information is required as described in Table 3. The problem dimension reflects the numbers of parameters to be optimized. The upper and lower limit sets for input weight and bias are 0 to 1, and the upper and lower limit sets for the number of hidden neurons are 2 to 200. The optimizer will assign default values to other parameters as required. The HOA optimization result had been compared with commonly used optimizers, which are genetic algorithm (GA), particle swarm optimization (PSO), and whale optimization algorithm (WOA). Figure 5 shows the optimization results for CWRU datasets using the D2 configuration. The GA optimizer was able to find the minimum solution at 32 iterations, PSO optimizer found the minimum solution at 31 iterations, WOA

optimizer found the minimum solution at 23 iterations, and HOA optimizer found the solution at 26 iterations. The HOA optimizer provides competitive performance with the WOA optimizer in finding the minimum solution for the CWRU dataset. The same optimizer parameter value described in Table 3 is used in order to find the minimum solution for experimental datasets using configuration D4 (see Table 2). The result is shown in Figure 6.

Based on the result, the HOA optimizer outperformed the other optimizer by finding the minimum solution at 18 iterations, while GA found the minimum solution at 59 iterations, PSO found the minimum solution at 42 iterations, and WOA found the minimum solution at 31 iterations. The optimized ELM parameter values were then extracted from the optimizer accordingly and summarized in Table 4. All these values were then set in the ELM and run for fault classification. For conversion from integer into matrix for input weight and bias, Equations 10 and 11 were used.

$$w_{opt,max} = w_{opt} \times 2 \quad w_{opt,min} = \frac{w_{opt}}{2} \quad (10)$$

$$b_{opt,max} = b_{opt} \times 2 \quad b_{opt,min} = \frac{b_{opt}}{2} \quad (11)$$

Fault classification result

This section employs the proposed IELM-HOA for fault classification purposes. The result will also be compared with conventional-ELM methods and recent methods, which are ELM-GA, ELM-PSO, and ELM-WOA, accordingly. All the optimized value in Table

Table 3. HOA parameter value

Description	Value
Number of search agent	500
Problem dimension	3
Upper limit	[1 1 200]
Lower limit	[0 0 2]
Number of iterations	100
Others	Deafult values

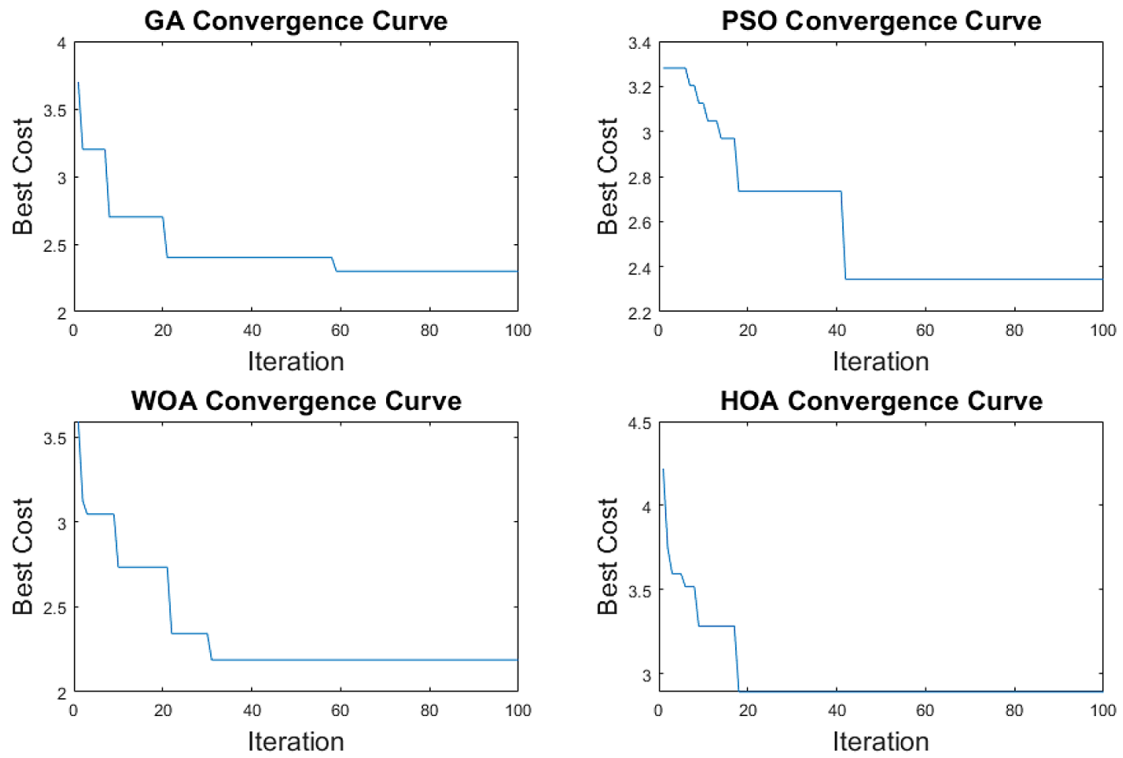**Figure 6.** Experimental optimization result for GA, PSO, WOA and HOA
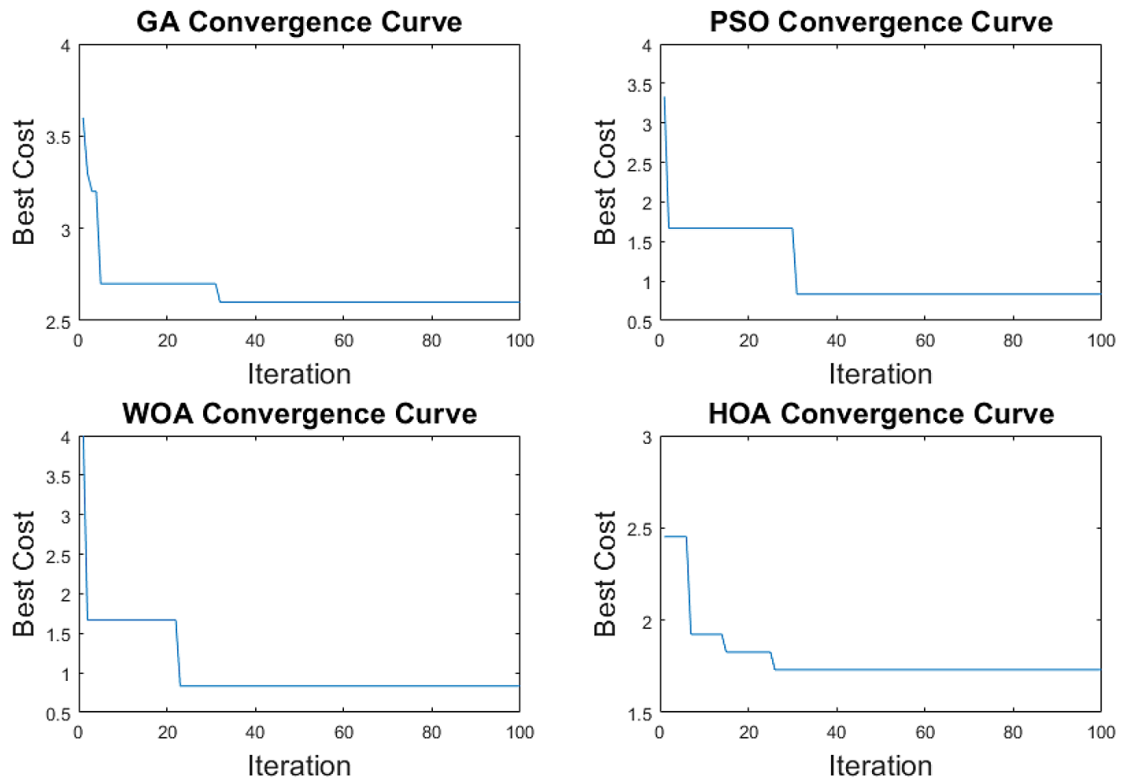

Figure 5. CWRU optimization result for GA, PSO, WOA and HOA

4 and configurations D1 and D3 were used in the IELM-HOA setup. We ran all the diagnostic approaches in this study 30 times. Figures 7 and 8 present the results for CWRU datasets and experimental datasets. Based on the result, the classification results for IELM-HOA show

Table 4. The optimized ELM parameters values

Datasets	Optimizer	Input weight	Bias	No. of hidden neurons
CWRU	GA	0.98	0.28	183
	PSO	0.42	0.51	106
	WOA	0.10	0.41	85
	HO	0.80	0.71	194
Experiment	GA	0.94	0.50	188
	PSO	0.50	0.10	159
	WOA	0.50	0.61	197
	HO	0.66	0.45	195
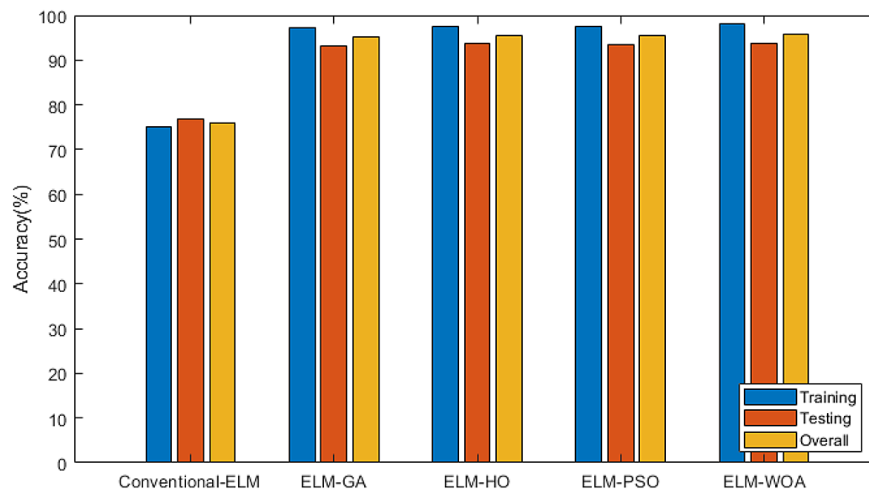
Figure 7. Classification accuracy for different diagnostic approaches for CWRU datasets

Figure 8. Classification accuracy for different diagnostic approaches for experimental datasets

competitive performance with other optimized-ELM approaches using GA, PSO, and WOA. As compared with conventional ELM, it provides almost 5–10% better classification performance. This result was expected, as the CWRU datasets considered clean signals, as the differences
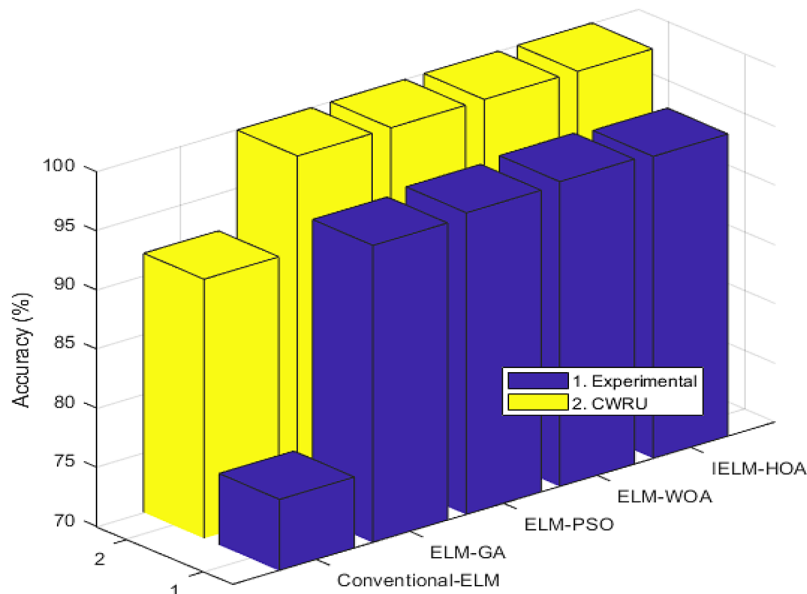
Table 5. Classification accuracy for different diagnosis approaches for CWRU datasets

Run	Approaches									
	A_Tr	A_Te	B_Tr	B_Te	C_Tr	C_Te	D_Tr	D_Te	E_Tr	E_Te
1	88.8	81.0	100	100	100	100	100	100	100	100
2	87.4	82.0	100	100	100	100	100	100	100	100
3	86.8	81.0	100	100	100	100	100	100	100	100
4	89.8	77.0	100	100	100	100	100	100	100	100
5	90.0	82.0	100	100	100	100	100	100	100	100
6	90.6	84.0	100	100	100	100	100	100	100	100
7	90.0	84.0	100	100	100	100	100	100	100	100
8	86.8	82.0	100	100	100	100	100	100	100	100
9	89.2	83.0	100	100	100	100	100	100	100	100
10	90.2	84.0	100	100	100	100	100	100	100	100
11	84.4	79.0	100	100	100	100	100	100	100	100
12	80.4	78.0	100	100	100	100	100	100	100	100
13	89.0	79.0	100	100	100	100	100	100	100	100
14	90.2	83.0	100	99.2	100	100	100	100	100	100
15	89.6	81.0	100	100	100	100	100	100	100	100
16	89.0	81.0	100	100	100	100	100	100	100	100
17	82.6	74.0	100	100	100	100	100	100	100	100
18	89.4	81.0	100	100	100	100	100	100	100	100
19	91.0	81.0	100	100	100	100	100	100	100	100
20	86.4	83.0	100	100	100	100	100	100	100	100
21	90.2	86.0	100	100	100	100	100	100	100	100
22	88.8	78.0	100	100	100	100	100	100	100	100
23	87.8	76.0	100	100	100	100	100	100	100	100
24	86.4	83.0	100	100	100	100	100	100	100	100
25	91.6	84.0	100	100	100	100	100	100	100	100
26	86.4	83.0	100	100	100	100	100	100	100	100
27	88.2	77.0	100	100	100	100	100	100	100	100
28	88.6	80.0	100	99.2	100	100	100	100	100	100
29	87.6	80.0	100	100	100	100	100	100	100	100
30	90.6	83.0	100	100	100	99.2	100	100	100	100
Average	88.3	81.0	100	99	100	99	100	100	100	100
Overall	84.7		99.5		99.5		100		100	

between signals seem significant, which enable the classification to go from nearly 99% to 100% classification accuracy for training, testing, and overall using the ELM-GA, ELM-PSO, ELM-WOA, and IELM-HOA approaches.

For experimental datasets, IELM-HOA is also able to compete with other optimized ELM approaches and provide significant improvement as compared with conventional ELM with 15–20% better classification performance. For IELM-HOA compared with ELM-GA, ELM-PSO, and ELM-WOA, the proposed method is able to provide around 1–2% better

performance. Figure 9, Table 5, and Table 6 present the details of accuracy recorded for each approach for both datasets, where A represents conventional-ELM, B represents ELM-GA, C represents ELM-PSO, D represents ELM-WOA, and E represents IELM-HOA accordingly. The terms Tr and Te represent the training and testing accordingly.

Overall, the CWRU datasets did not show any significant difference in terms of classification accuracy performance between ELM-GA, ELM-PSO, ELM-WOA, and IELM-HOA, as all of these approaches provided almost 100%

Table 6. Classification accuracy for different diagnosis approaches for experimental datasets

Run	Approaches									
	A_Tr	A_Te	B_Tr	B_Te	C_Tr	C_Te	D_Tr	D_Te	E_Tr	E_Te
1	88.8	81.0	95.6	92.5	97.5	93.1	98.1	93.1	96.4	92.5
2	87.4	82.0	97.5	93.1	97.8	93.1	97.7	93.1	97.7	93.8
3	86.8	81.0	97.3	93.8	97.5	92.5	98.4	95.0	97.5	93.1
4	89.8	77.0	96.9	93.1	98.0	93.8	97.7	94.4	97.8	93.1
5	90.0	82.0	96.6	93.1	97.8	92.5	98.0	94.4	97.3	93.1
6	90.6	84.0	97.2	93.1	97.7	92.5	98.1	95.0	98.3	92.5
7	90.0	84.0	97.0	91.9	97.3	91.9	98.0	93.1	97.0	92.5
8	86.8	82.0	96.6	94.4	97.8	93.1	98.1	93.1	97.8	93.1
9	89.2	83.0	96.9	93.1	97.7	94.4	98.1	94.4	97.7	92.5
10	90.2	84.0	97.2	93.1	97.7	92.5	97.8	92.5	97.8	93.8
11	84.4	79.0	97.2	93.8	97.5	93.8	98.0	93.1	98.0	95.0
12	80.4	78.0	96.7	93.1	97.3	94.4	98.3	95.6	97.7	93.8
13	89.0	79.0	97.2	93.1	97.3	92.5	98.1	92.5	97.8	93.8
14	90.2	83.0	97.3	93.1	97.8	92.5	97.8	93.8	97.5	93.1
15	89.6	81.0	97.3	95.0	97.5	93.8	97.8	93.8	97.3	93.1
16	89.0	81.0	97.2	92.5	98.1	94.4	97.8	93.1	98.0	94.4
17	82.6	74.0	97.3	91.9	97.2	94.4	98.3	92.5	97.7	94.4
18	89.4	81.0	97.7	93.1	97.3	93.1	98.4	93.1	97.2	93.8
19	91.0	81.0	97.0	93.1	97.7	94.4	98.0	96.3	97.0	94.4
20	86.4	83.0	97.2	93.1	97.2	94.4	98.3	94.4	97.5	91.9
21	90.2	86.0	97.3	93.1	97.7	92.5	97.5	92.5	98.7	94.4
22	88.8	78.0	97.2	91.9	97.8	93.1	98.4	95.0	98.0	93.8
23	87.8	76.0	97.5	92.5	97.3	93.8	98.3	93.1	97.5	95.0
24	86.4	83.0	97.0	93.	97.7	93.8	97.5	92.5	97.8	94.4
25	91.6	84.0	97.3	93.8	97.8	93.8	98.1	93.1	96.9	93.8
26	86.4	83.0	97.7	91.9	97.5	93.8	97.7	93.1	97.3	94.4
27	88.2	77.0	97.5	93.8	97.7	93.1	98.0	93.1	97.0	94.4
28	88.6	80.0	97.3	94.4	97.8	94.4	97.8	93.1	97.3	93.8
29	87.6	80.0	97.0	93.8	98.0	93.8	97.8	93.1	97.7	93.8
30	90.6	83.0	97.2	93.1	97.8	95.0	98.0	93.1	97.0	93.8
Average	88.3	81.0	97.2	93.2	97.6	93.5	98.0	93.6	98.5	93.6
Overall	84.7		95.2		95.6		95.8		96.1	

classification accuracy, but this approach shows significant improvement compared to conventional-ELM with an overall improvement in classification accuracy of 15 %. The experimental datasets also did not show any significant difference between ELM-GA, ELM-PSO, ELM-WOA, and IELM-HOA, but these approaches significantly outperform the conventional ELM with an overall improvement in classification accuracy of 10 %. Compared to other diagnosis approaches, the IELM-HOA achieved the highest classification accuracy of 96.1%. Based on these results, the optimization of the ELM

parameters is crucial to enhance and improve the overall performance of the ELM method

CONCLUSIONS

This paper presents a novel approach to machine reliability assessment, utilizing enhanced ELM, which is founded on the HOA method. The HOA method was used to select the parameters for the ELM method, particularly the input weight, bias, and number of hidden neurons. A simplified machinery equipment was used for
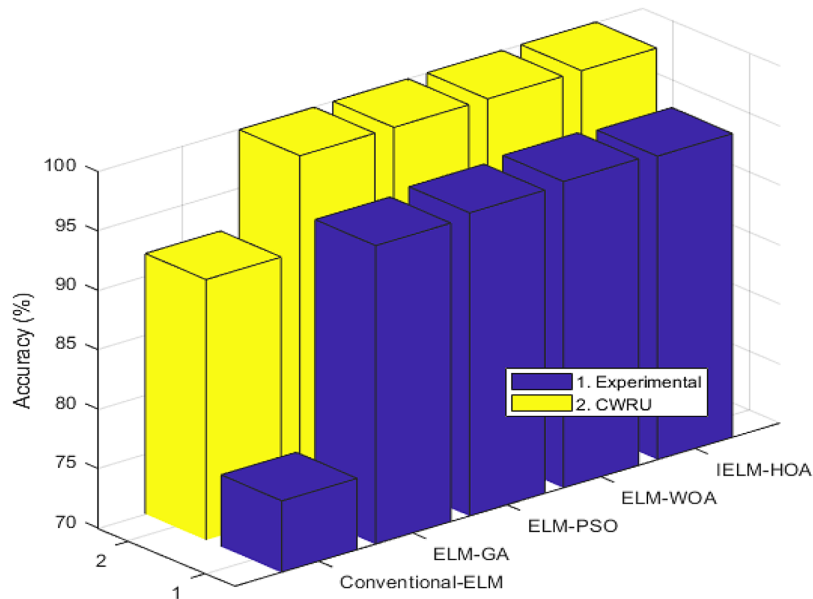
Figure 9. Overall comparison of the diagnosis approaches

experiments, and the proposed method was also tested with online CWRU bearing datasets. Here is a summary of the study's findings:

- The HOA method proved its capability to optimize the ELM method by selecting an accurate input weight, bias, and hidden neurons.
- The proposed IELM-HOA provides an effective and efficient rotating machinery fault diagnosis approach as compared with conventional-ELM and competitive performance with approximately 5–15% better classification performance.

We could test the proposed IELM-HOA on various components, including blades and shafts, in future work. We will also test our proposed method's capability and suitability to be implemented in transfer learning studies.

Acknowledgments

REFERENCES

1. Zhang Y, Shang L, Gao H, He Y, Xu X, Chen Y. A new method for diagnosing motor bearing faults based on Gramian angular field image coding and improved CNN-ELM. IEEE Access 2023; 11: 11337–11349.

2. Chen Y, Yuan Z, Chen J, Sun K. A novel fault diagnosis method for rolling bearing based on hierarchical refined composite multiscale fluctuation-based dispersion entropy and PSO-ELM. Entropy. 2022. https://doi.org/10.3390/e24111517

3. Hu Y, Wei R, Yang Y, Li X, Huang Z, Liu Y, He C, Lu H. Performance degradation prediction using LSTM with optimized parameters. Sensors. 2022. https://doi.org/10.3390/s22062407

4. Meng Z, Zhang Y, Zhu B, Pan Z, Cui L, Li J, Fan F. Research on rolling bearing fault diagnosis method based on ARMA and optimized MOMEDA. Measurement (Lond). 2022. https://doi.org/10.1016/j.measurement.2021.110465

5. Wei H, Zhang Q, Shang M, Gu Y. Extreme learning Machine-based classifier for fault diagnosis of rotating Machinery using a residual network and continuous wavelet transform. Measurement (Lond). 2021. https://doi.org/10.1016/j.measurement.2021.109864

6. Qiu Z, Yuan X, Wang D, Fan S, Wang Q. Physical model driven fault diagnosis method for shield Machine hydraulic system. Measurement (Lond). 2023. https://doi.org/10.1016/j.measurement.2023.113436

7. Wang S, Tian J, Liang P, Xu X, Yu Z, Liu S, Zhang D. Single and simultaneous fault diagnosis of gearbox via wavelet transform and improved deep residual network under imbalanced data. Eng Appl Artif Intell. 2024. https://doi.org/10.1016/j.engappai.2024.108146

8. Sun C, Wang Y, Sun G. A multi-criteria fusion feature selection algorithm for fault diagnosis of helicopter planetary gear train. Chinese Journal of Aeronautics 2020; 33: 1549–1561.

9. Guo J, Li X, Lao Z, Luo Y, Wu J, Zhang S. Fault diagnosis of industrial robot reducer by an extreme learning machine with a level-based learning swarm optimizer. Advances in Mechanical Engineering. 2021. https://doi.org/10.1177/16878140211019540

10. Liu X, Huang H, Xiang J. A personalized diagnosis method to detect faults in gears using numerical simulation and extreme learning machine. Knowl Based Syst 2020; 195: 105653.

11. Huang G Bin, Zhu QY, Siew CK. Extreme learning machine: Theory and applications. Neurocomputing 2006; 70: 489–501.

12. Deo A, Pandey I, Khan SS, Mandlik A, Doohan NV, Panchal B. deep learning-based red blood cell classification for sickle cell anemia diagnosis using hybrid CNN-LSTM model. Traitement du Signal 2024; 41: 1293–1301.

13. Sheini Dashtgoli D, Taghizadeh S, Macconi L, Concli F. Comparative analysis of machine learning models for predicting the mechanical behavior of bio-based cellular composite sandwich structures. Materials. 2024. https://doi.org/10.3390/ma17143493

14. Yousuf SM, Khan MA, Ibrahim SM, Sharma AK, Ahmad F, Kumar P. A comparison of experimental and computational methods for circular footing response on lime-treated geotextile reinforced silty sand. Model Earth Syst Environ. 2024; 10: 1281–1303

15. Cao L, Sun W. Research on Bearing Fault Identification of Wind Turbines' Transmission System Based on Wavelet Packet Decomposition and Probabilistic Neural Network. Energies, 2024. https://doi.org/10.3390/en17112581

16. Meng L, Liu M, Wei P, Qin H. Rolling Bearing Fault Diagnosis Based on Improved VMD And GA-ELM. In: Peng C, Sun J (eds) 2021 Proceedings of the 40th Chinese Control Conference (CCC). 2021, 4414–4419.

17. Guo L, Qian J. Rolling Bearing Fault Diagnosis Based on QGA Optimized DBN-ELM Model. In: 2023 35TH Chinese control and decision conference, CCDC. 2023; 5466–5473.

18. Isham MF, Leong MS, Lim MH, Ahmad ZAB Optimized ELM based on Whale Optimization Algorithm for gearbox diagnosis. MATEC Web Conf. 2019; 255.

19. Isham MF, Saufi MSR, Waziralilah NF, Talib MHAb, Hasan MDA, Saad WAA Optimized-ELM Based on Geometric Mean Optimizer for Bearing Fault Diagnosis. In: Mohd. Isa WH, Khairuddin IMohd, Mohd. Razman MohdA, Saruchi S 'Atifah, Teh S-H, Liu P (eds) Intelligent Manufacturing and Mechatronics. Springer Nature Singapore, Singapore, 2024; 125–139.

20. Wang J, Zhang Y, Zhang F, Li W, Lv S, Jiang M, Jia L. Accuracy-improved bearing fault diagnosis method based on AVMD theory and AWPSO-ELM model. Measurement 2021; 181: 109666.

21. Sun Z, Mu L, Li F, Wei N, Wang Y, Wu S, Lei M, Liu Q. Vibration Fault Diagnosis of Circuit Breaker Based on CGWO-VMD and ELM Combined with PCA. In: 2022 4th International Conference on Smart Power & Internet Energy Systems (SPIES). 2022; 1237–1242.